Comparison of Spectroscopic Strategies to Determine Molecular Geometries and the Impact of Nuclear versus Atomic Masses: The Example of HCO + and HOC +

Mirjana Mladenovic, Marius Lewerenz

Comparison of Spectroscopic Strategies to Determine Molecular Geometries and the Impact of Nuclear versus Atomic Masses: The Example of HCO^+ and HOC^+

Mirjana Mladenović* and Marius Lewerenz†
Université Paris-Est, Laboratoire Modélisation et Simulation Multi-Echelle (MSME), UMR 8208 CNRS, 5 bd Descartes, 77454 Marne la Vallée, France
(Dated: to appear in a special issue of the journal Molecular Physics devoted to the 25th HRMS Colloquium, 2018)

We compare a recently proposed mixed experimental/theoretical procedure for the derivation of molecular equilibrium structures with several commonly used spectroscopic approaches using experimental data for several isotopologues. We also examine the sensitivity of the results from these approaches to the replacement of the commonly employed atomic masses with nuclear masses. This point is of particular importance for ionic species like HCO^+ and HOC^+ which serve as numerical reference cases. The scatter of molecular equilibrium geometries derived by different approaches is found to exceed stated statistical uncertainties by about an order of magnitude.

I. INTRODUCTION

Recently, standard spectroscopic parameters for the isotopologues of HCO^+ and HOC^+ were determined by means of a theoretical two-step procedure.[1] In the first step, the *ab initio* computed three-dimensional CCSD(T)/cc-pVQZ potential energy surface of Mladenović and Schmatz[2] for the isomerizing system HCO^+/HOC^+ was used to obtain the energies of the rotational levels up to $J = 15$ in the ground vibrational state and in the singly excited vibrational ν_i states for $i = 1 - 3$. The computed rovibrational energies were fitted to the conventional spectroscopic expressions. The rotational constants $B_i^{\rm th}$ obtained in this manner for $i = 0 - 3$ deviate by approximately $0.005\,{\rm cm}^{-1}(200\,{\rm MHz})$ from their experimentally derived counterparts $B_i^{\rm exp}$. This disagreement was corrected in the second step. Ascribing the difference between $B_i^{\rm th}$ and $B_i^{\rm exp}$ to the restricted accuracy of the equilibrium bond lengths, a new set of structural parameters was derived by combining the experimental ground-state rotational constants $B_0^{\rm exp}$ with theoretical rotation-vibration corrections $\Delta B_0^{\rm th} = B_e^{\rm th} - B_0^{\rm th}$ computed variationally (beyond a perturbational approach), where $B_e^{\rm th}$ is the equilibrium rotational constant for the CCSD(T)/cc-pVQZ potential energy surface. The procedure introduced in Ref. 1, hereafter Paper I, led to estimates of the spectroscopic constants and equilibrium bond distances in excellent agreement with values derived from experiments.

All stable isotopologues of HCO^+ and HOC^+ involving H, D, ^{16}O, ^{17}O, ^{18}O, ^{12}C, and ^{13}C were considered in Paper I, in total 24 molecular cations. The rovibrational calculations and the equilibrium structure determinations were carried out using atomic masses. This is common practice in nuclear dynamics computations, but there is an obvious problem for ionic species.

Within the Born-Oppenheimer approximation, interacting nuclei are described by a mass-independent potential energy (hyper)surface, providing the energy of the electronic subsystem, so that a single potential energy surface is used for all isotopic variants of a molecular system under investigation. The equilibrium geometry, defined as usual as the minimum of the potential energy surface, is thus mass-independent and unique for all isotopologues. The Born-Oppenheimer approximation and its electronic-structure implementations rely on a perfect separation of the electronic and nuclear coordinates. This, in turn, implies that the nuclear (rotation-vibrational) motion should, rigorously speaking, involve the nuclear masses. Whereas the use of atomic masses in connection with nuclear dynamics computations is considered to be a pragmatic approach, the use of nuclear masses is conceptually more correct and the only sound basis for systematic improvements.

The purpose of the present paper is to investigate the influence of the nuclear versus atomic masses on the spectroscopic and structural parameters of the molecular cations HCO^+ and HOC^+. Since the masses explicitly enter in the process of extracting the geometric parameters from the observed spectral (rotational) transitions, this issue is of relevance also for estimating equilibrium structures from experimental ground-state rotational constants. In practice, rotational transitions observed for linear triatomic molecules are compactly represented by a polynomial expansion in terms of $J(J+1)$ and K^2, where J and K are the quantum numbers specifying the state of the total rotational angular momentum and of its projection onto the body-fixed (molecular) z axis, respectively. The frequency ν of the rotational transition $J \to J+1$ in a vibrational Σ state v is, for instance, given by

$$\begin{aligned}\nu =& 2\,B_v\,(J+1) - 4\,D_v\,(J+1)^3 \\ &+ 2\,H_v\,(J+1)^3(3J^2+6\,J+4)\ldots\,,\end{aligned} \tag{1}$$

where B_v, D_v, H_v, and so on, are expansion parameters appropriate for the vibrational state v. The dominant term in Eq. (1) is the first term involving the rotational constant B_v. For a given geometric arrangement or a rigid body, the rotational constant is a quantity well-established from the mathematical and physical point of view. In the actual circumstances of rotating and vibrating systems, we do, however, encounter problems of both conceptual and practical nature.[3–8] In the present work, we revisit some of these issues on the example of HCO^+

TABLE I: Atomic m_a and nuclear m_n masses in the unified atomic mass unit u.[a] The reduced masses μ_r, μ_R (in u) for the main form of HCO^+ are calculated by means of Eq. (8).

species	m_a	m_n
H	1.007825035	1.0072765
D	2.014101779	2.0135532
^{12}C	12.0	11.9967085
^{13}C	13.003354826	13.0000633
^{16}O	15.99491463	15.9905260
^{18}O	17.99916030	17.9947717
μ_r	6.856209	6.854328
μ_R	0.972804	0.972283

[a] The atomic masses are taken from Ref. 9.

and HOC^+. We first give a brief overview of the theoretical approach which we employed (Section II). Our quantum-mechanical calculations provide a consistent set of data, which we use to study the mass effect on spectral and geometric parameters (Section II A). Different commonly used approaches to obtain information about the equilibrium structure are considered (Section III), leading us to a certain number of conclusions (Section IV).

II. SPECTRAL AND GEOMETRIC PARAMETERS

The theoretical approach of Paper I is used in combination with nuclear masses in this work. Masses are given in the unified atomic mass unit u, which stands for u=m$_a$(^{12}C)/12=10^{-3} kg mol^{-1}/N$_A$, where m$_a$(^{12}C) is the mass of the atom ^{12}C and N_A Avogadro's number.[9] The atomic (nuclear plus electronic) masses m_a and the nuclear masses m_n of the isotopes of hydrogen, carbon, and oxygen are summarized in Table I for convenience. A glance at Table I shows that m_n are approximately 5×10^{-4} to 5×10^{-3} u (0.05 %) smaller than m_a. In our computations, the nuclear masses are internally evaluated from the atomic masses m_a provided in Table I. The conversion factor used for the electron mass is 1822.888515, so that $m_e = 1/1822.888515$ u.

In our present analysis, we include only those isotopologues of HCO^+ and HOC^+, for which experimental values of the ground-state rotational constant $B_0^{\rm exp}$ are known. This is the case for eight substituted isotopic forms of HCO^+ (HCO^+,[10] $HC^{17}O^+$,[11] $HC^{18}O^+$,[12] $H^{13}CO^+$,[13] $H^{13}C^{18}O^+$,[14] DCO^+,[15] $DC^{18}O^+$,[16] and $D^{13}CO^+$ [13]) and four isotopologues of HOC^+ (HOC^+,[17] $H^{18}OC^+$,[18] $HO^{13}C^+$,[18,19] and DOC^+ [17]).

squeezetable

The rovibrational energies computed using the nuclear masses for the total rotational angular momentum up to $J = 15$ are fitted to appropriate spectroscopic formulae, following the procedure of Paper I. To facilitate the comparison, the same effective spectroscopic Hamiltonians are used for the atomic-mass and nuclear-mass cases for each of the species studied. The spectroscopic parameters obtained in the fits for the vibrational ground state and for the singly excited ν_1, ν_2, and ν_3 states are listed in Tables II and III for the isotopic variants of HCO^+ and in Table IV for the isotopic variants of HOC^+. There, T_v is the term energy and B_v the effective rotational constant for the vibrational state v, where we use $v = 0 - 3$ to denote the vibrational states $(0, 0^0, 0)$, $(1, 0^0, 0)$, $(0, 1^1, 0)$, and $(0, 0^0, 1)$, respectively. The centrifugal distortion contribution is expressed in terms of the quartic centrifugal distortion constant D_v and higher order constants, such as H_v (sextic), L_v (octic), and so on. The ℓ-type doubling contribution is described by the ℓ-type doubling constant q_v and the parameters q_v^J, q_v^{JJ}, and so on for its centrifugal distortion corrections. The results obtained using the atomic masses are taken from Paper I. The equilibrium rotational constants and effective rotational constants computed using atomic masses are denoted by B_e^a and B_v^a, respectively. Qualities of the fits obtained in the atomic-mass and nuclear-mass cases are comparable, as seen by similar fit standard deviations σ of approximately 10 Hz in Tables II-IV.

The replacement of the atomic masses with the nuclear masses affects the effective rotational constants B_0, B_1, B_2, B_3 by 9-15 MHz, as seen by inspection of the difference $B_v - B_v^a$ in Tables II-IV. There we also see that the difference $B_e - B_e^a$ is equal to 9-15 MHz, too, where B_e and B_e^a are the equilibrium rotational constants computed for the CCSD(T)/cc-pVQZ equilibrium structure using nuclear masses and atomic masses, respectively. This thus shows that the difference $B_e - B_e^a$ is a major contributor to the difference $B_v - B_v^a$ for $v = 0 - 3$. The centrifugal distortion constants D_v are approximately 0.05 kHz (0.05 %) larger than D_v^a. The ℓ-type doubling constants q_v are larger than q_v^a by 0.1 MHz for the isotopic forms of HCO^+ and by 0.2 MHz for the isotopic forms of HOC^+, which represent a change of approximately 0.05 %. The vibration-rotation interaction constants $\alpha_v = B_0 - B_v$ are larger than $\alpha_v^a = B_0^a - B_v^a$ by at most 0.2 MHz (0.05 %). Finally, the wavenumbers of the ν_1, ν_2, ν_3 vibrations are increased by at most 1 cm^{-1} upon replacement of atomic masses with nuclear masses.

After publication of Paper I, we have learned that Warner in his Ph.D. thesis[14] had measured the rotational transitions $J = 2 \rightarrow 3$ and $J = 3 \rightarrow 4$ in the ground vibrational state of HOC^+, $H^{18}OC^+$, and $HO^{13}C^+$, from which he had derived $(B_0^{\rm exp}, D_0^{\rm exp})$ of (44 743.943,116.75), (43 305.969,108.32), (42 876.559,107.25) in (MHz,kHz) for these systems, respectively. These results are in good agreement with the experimental data of Gudeman et al.[18,19] and Amano and Maeda,[17] which were used in Paper I (Table III) and here in Table IV. Warner had also measured the rotational transition $J = 2 \rightarrow 3$ at 248 459.964 MHz in the ground vibrational state of $H^{18}O^{13}C^+$. From this value using Eq. (1), one calcu-

TABLE II: Spectroscopic parameters derived for the isotopic variants of HCO^+ using nuclear masses. Values shown in brackets were obtained in Paper I using atomic masses.

Parameter	$H^{12}C^{16}O^+$	$H^{12}C^{17}O^+$	$H^{12}C^{18}O^+$	$H^{13}C^{16}O^+$	$H^{13}C^{18}O^+$
B_e / MHz	44635.23	43565.63	42614.46	43412.78	41361.54
$B_e - B_e^a$ / MHz	15.22	14.58	14.02	14.35	13.13
B_0 / MHz	44391.37	43330.07	42386.20	43178.57	41142.93
$B_0 - B_0^a$ / MHz	15.09	14.45	13.91	14.23	13.02
D_0 / kHz	82.01 [81.95]	78.15 [78.10]	74.81 [74.76]	77.64 [77.59]	70.56 [70.51]
H_0 / Hz	0.071 [0.071]	0.065 [0.065]	0.061 [0.061]	0.063 [0.063]	0.053 [0.053]
σ_0 / Hz	9.70 [8.45]	8.93 [8.81]	9.34 [7.63]	8.17 [8.93]	5.82 [6.90]
$B_0^{\rm est}$ / MHz	44594.46 [44594.42]	43528.43 [43528.77]	42580.37 [42580.99]	43376.53 [43377.18]	41331.84 [41333.14]
$B_0^{\rm exp}$ / MHz	44594.42866(16)[a]	43528.9253(19)[b]	42581.21(4)[c]	43377.3019(17)[d]	41333.587(5)[e]
T_2 /cm^{-1}	829.44 [829.25]	828.40 [828.21]	827.48 [827.29]	821.98 [821.80]	820.01 [819.82]
B_2 / MHz	44471.56	43407.86	42461.87	43249.54	41209.65
$B_2 - B_2^a$ / MHz	15.11	14.47	13.93	14.25	13.03
D_2 / kHz	83.62 [83.57]	79.67 [79.62]	76.24 [76.19]	79.06 [79.01]	71.81 [71.76]
H_2 / Hz	0.084 [0.084]	0.077 [0.077]	0.071 [0.071]	0.074 [0.074]	0.062 [0.062]
σ_2 / Hz	12.33 [11.45]	10.17 [9.81]	9.02 [8.45]	9.60 [9.64]	7.95 [8.02]
q_2 / MHz	209.95 [209.85]	200.30 [200.21]	191.90 [191.82]	200.44 [200.36]	182.47 [182.40]
q_2^J / kHz	-1.80 [-1.79]	-1.67 [-1.67]	-1.56 [-1.56]	-1.65 [-1.65]	-1.42 [-1.42]
q_2^{JJ} / Hz	0.024 [0.024]	0.022 [0.022]	0.019 [0.019]	0.020 [0.020]	0.016 [0.016]
σ_q / Hz	9.68 [9.14]	9.65 [9.69]	7.68 [6.15]	7.89 [9.07]	6.68 [6.39]
α_2 / MHz	-80.19 [-80.17]	-77.79 [-77.77]	-75.68 [-75.66]	-70.97 [-70.95]	-66.72 [-66.70]
$B_2^{\rm est}$ / MHz	44674.65 [44674.59]	43606.24 [43606.54]	42656.06 [42656.65]	43447.52 [43448.13]	41398.57 [41399.84]
$B_2^{\rm exp}$ / MHz	44677.1489(18)[d]		42659.160(8)[e]	43450.524(8)[e]	41402.389(8)[e]
T_3 /cm^{-1}	2179.44 [2179.09]	2152.65 [2152.31]	2128.52 [2128.19]	2145.68 [2145.35]	2092.82 [2092.51]
B_3 / MHz	44098.63	43047.00	42111.71	42895.00	40877.89
$B_3 - B_3^a$ / MHz	14.94	14.30	13.76	14.08	12.89
D_3 / kHz	82.10 [82.04]	78.24 [78.18]	74.88 [74.83]	77.74 [77.69]	70.64 [70.59]
H_3 / Hz	0.070 [0.070]	0.065 [0.065]	0.060 [0.060]	0.062 [0.062]	0.053 [0.053]
σ_3 / Hz	7.88 [7.51]	6.60 [7.25]	6.40 [5.62]	7.44 [7.10]	5.39 [5.57]
α_3 / MHz	292.75 [292.59]	283.07 [282.91]	274.49 [274.34]	283.57 [283.42]	265.04 [264.90]
$B_3^{\rm est}$ / MHz	44301.71 [44301.83]	43245.38 [43245.85]	42305.90 [42306.65]	43092.98 [43093.76]	41066.81 [41068.24]
$B_3^{\rm exp}$ / MHz	44299.8687(78)[d]		42305.024(8)[e]	43091.852(8)[e]	
T_1 /cm^{-1}	3086.29 [3085.58]	3083.79 [3083.08]	3081.67 [3080.96]	3063.70 [3062.99]	3059.76 [3059.05]
B_1 / MHz	44038.81	42986.42	42051.39	42850.77	40834.08
$B_1 - B_1^a$ / MHz	14.94	14.31	13.77	14.09	12.91
D_1 / kHz	81.27 [81.22]	77.48 [77.42]	74.16 [74.12]	77.03 [76.98]	69.98 [69.93]
H_1 / Hz	0.068 [0.068]	0.065 [0.065]	0.061 [0.061]	0.062 [0.062]	0.054 [0.054]
σ_1 / Hz	15.18 [14.70]	13.25 [13.28]	10.83 [9.41]	9.88 [9.38]	8.97 [9.49]
α_1 / MHz	352.57 [352.41]	343.65 [343.51]	334.81 [334.67]	327.80 [327.66]	308.86 [308.74]
$B_1^{\rm est}$ / MHz	44241.89 [44242.01]	43184.80 [43185.26]	42245.58 [42246.32]	43048.75 [43049.52]	41023.00 [41024.39]
$B_1^{\rm exp}$ / MHz	44240.53309(56)[e]		42244.862(8)[e]	43048.158(8)[e]	
${}^{(n)}B_e^{\rm est}[{}^{(a)}B_e^{\rm est}]$/ MHz	44838.30 [44838.15]	43763.99 [43764.21]	42808.63 [42809.14]	43610.75 [43611.28]	41550.44 [41551.63]
${}^{(a)}B_e^{\rm exp}$ / MHz	44840.1330(161)[g]		42811.0181(161)[g]	43613.2505(161)[g]	
$S_0[S_0^a]$ /MHz	242.47 [242.33]	235.57 [235.44]	228.97 [228.85]	234.72 [234.59]	220.23 [220.12]
ΔB_0 / MHz	243.86 [243.73]	235.56 [235.44]	228.27 [228.15]	234.22 [234.10]	218.61 [218.50]
$\Delta B_0 - S_0$ / MHz	1.39	-0.01	-0.70	-0.50	-1.62

[a] Fit 2 of Cazzoli et al.[10]
[b] Dore et al.[11]
[c] Bogey et al.[12]
[d] Lattanzi et al.[13]
[e] Warner.[14]
[f] Neese et al.[20]
[g] Dore et al.[15]

TABLE III: Spectroscopic parameters derived for the isotopic variants of DCO^+ using nuclear masses. Values shown in brackets were obtained in Paper I using atomic masses.

Parameter	$D^{12}C^{16}O^+$	$D^{12}C^{18}O^+$	$D^{13}C^{16}O^+$
B_e / MHz	36035.19	34424.09	35379.38
$B_e - B_e^a$ / MHz	9.86	9.02	9.52
B_0 / MHZ	35861.59	34261.63	35210.56
$B_0 - B_0^a$ / MHz	9.78	8.96	9.45
D_0 / kHz	55.24 [55.21]	50.16 [50.13]	52.88 [52.85]
H_0 / Hz	0.050 [0.050]	0.043 [0.043]	0.046 [0.046]
σ_0 / Hz	6.76 [6.56]	4.99 [5.54]	6.19 [6.18]
$B_0^{\rm est}$ / MHz	36020.07 [36019.81]	34413.35 [34413.66]	35366.58 [35366.70]
$B_0^{\rm exp}$ / MHz	36019.76765(14)[a]	34413.78556(18)[a]	35366.70968(21)[a]
T_2 /cm^{-1}	666.39 [666.30]	663.90 [663.81]	656.94 [656.85]
B_2 / MHz	35956.82	34352.11	35297.88
$B_2 - B_2^a$ / MHz	9.83	9.00	9.48
D_2 / kHz	56.85 [56.82]	51.59 [51.56]	54.33 [54.30]
H_2 / Hz	0.063 [0.063]	0.054 [0.054]	0.058 [0.058]
σ_2 / Hz	12.75 [12.29]	8.55 [8.19]	8.30 [7.76]
q_2 / MHz	169.63 [169.56]	155.42 [155.36]	165.82 [165.76]
q_2^J / kHz	-1.32 [-1.32]	-1.15 [-1.15]	-1.25 [-1.25]
q_2^{JJ} / Hz	0.023 [0.023]	0.019 [0.019]	0.021 [0.021]
σ_q / Hz	5.18 [5.05]	7.50 [7.81]	9.66 [9.44]
α_2 / MHz	-95.22 [-95.18]	-90.48 [-90.45]	-87.32 [-87.29]
$B_2^{\rm est}$ / MHz	36115.30 [36115.00]	34503.83 [34504.10]	35453.90 [35453.98]
$B_2^{\rm exp}$ / MHz	36116.66634(80)[b]		
T_3 /cm^{-1}	1901.07 [1900.81]	1870.99 [1870.75]	1894.10 [1893.85]
B_3 / MHz	35656.03	34071.61	35012.79
$B_3 - B_3^a$ / MHz	9.70	8.89	9.36
D_3 / kHz	55.21 [55.18]	50.11 [50.09]	52.84 [52.81]
H_3 / Hz	0.049 [0.049]	0.043 [0.043]	0.044 [0.044]
σ_3 / Hz	2.83 [2.44]	2.64 [3.00]	2.66 [2.54]
α_3 / MHz	205.56 [205.48]	190.02 [189.94]	197.77 [197.69]
$B_3^{\rm est}$ / MHz	35814.51 [35814.34]	34223.33 [34223.71]	35168.81 [35169.01]
$B_3^{\rm exp}$ / MHz	35813.3618(31)[b]		
T_1 /cm^{-1}	2580.80 [2580.46]	2554.57 [2554.23]	2529.79 [2529.47]
B_1 / MHz	35636.66	34010.18	34844.93
$B_1 - B_1^a$ / MHz	9.74	8.87	9.31
D_1 / kHz	46.08 [46.05]	40.54 [40.52]	40.32 [40.28]
H_1 / Hz	-2.444 [-2.441]	0.039 [0.039]	-4.001 [-4.004]
L_1 / mHz	0.328 [0.326]	-0.198 [-0.196]	1.508 [1.509]
K_1 /μHz	0.037 [0.037]	0.001 [-0.002]	-0.484 [-0.484]
σ_1 / Hz	4.12 [3.92]	8.33 [10.12]	16.47 [15.73]
α_1 / MHz	224.94 [224.89]	251.45 [251.36]	365.62 [365.50]
$B_1^{\rm est}$ / MHz	35795.13 [35794.93]	34161.90 [34162.30]	35000.95 [35001.20]
$B_1^{\rm exp}$ / MHz	35792.3325(46)[c]		
${}^{(n)}B_e^{\rm est}[{}^{(a)}B_e^{\rm est}]$ / MHz	36193.65 [36193.34]	34575.79 [34576.06]	35535.38 [35535.45]
${}^{(a)}B_e^{\rm exp}$ / MHz	36194.3538(79)[d]		
$S_0[S_0^a]$ /MHz	120.03 [120.00]	130.25 [130.21]	194.37 [194.30]
ΔB_0 / MHz	173.60 [173.53]	162.46 [162.40]	168.82 [168.75]
$\Delta B_0 - S_0$ / MHz	53.57	32.21	-25.55

[a] Caselli and Dore.[16]
[b] Hirao et al.[21]
[c] Lattanzi et al.[13]
[d] Dore et al.[15]

TABLE IV: Spectroscopic parameters derived for $H^{16}O^{12}C^+$, $H^{18}O^{12}C^+$, $H^{16}O^{13}C^+$, and $D^{16}O^{12}C^+$ using nuclear masses. Values shown in brackets were obtained in Paper I using atomic masses.

Parameter	$H^{16}O^{12}C^+$	$H^{18}O^{12}C^+$	$H^{16}O^{13}C^+$	$D^{16}O^{12}C^+$
B_e / MHz	44567.75	43156.82	42709.61	37877.31
$B_e - B_e^a$ / MHz	14.43	13.47	13.33	10.38
B_0 / MHz	44525.06	43091.57	42665.27	38024.35
$B_0 - B_0^a$ / MHz	14.31	13.35	13.23	10.42
D_0 / kHz	113.83 [113.76]	106.02 [105.96]	104.21 [104.14]	93.64 [93.59]
H_0 / Hz	0.076 [0.760]	0.579 [0.579]	0.619 [0.611]	2.306 [2.305]
L_0 / mHz	-0.046 [-0.046]	-0.032 [-0.032]	-0.034 [-0.034]	-0.245 [-0.245]
K_0 /μHz				0.025 [0.026]
σ_0 / Hz	3.40 [4.30]	3.32 [3.77]	3.53 [3.41]	0.74 [0.88]
$B_0^{\rm est}$ / MHz	44744.06 [44743.93]	43305.20 [43305.74]	42875.92 [42876.36]	38193.18 [38193.20]
$B_0^{\rm exp}$ / MHz	44743.9141(35)[a]	43305.969(35)[b]	42876.559(8)[b]	38193.1984(18)[a]
T_2 /cm^{-1}	243.67 [243.60]	241.15 [241.08]	243.30 [243.23]	176.60 [176.57]
B_2 / MHz	44719.37	43252.36	42845.08	38349.08
$B_2 - B_2^a$ / MHz	14.32	13.33	13.22	10.54
D_2 / kHz	116.23 [116.15]	107.84 [107.78]	106.39 [106.33]	100.69 [100.63]
H_2 / Hz	0.284 [0.284]	0.177 [0.177]	0.234 [0.235]	1.738 [1.734]
L_2 / mHz	0.028 [0.028]	0.026 [0.026]	0.021 [0.021]	-0.051 [-0.049]
K_2 /μHz				-0.011 [-0.012]
σ_2 / Hz	8.90 [8.38]	6.48 [6.46]	6.16 [6.72]	0.77 [1.02]
q_2 / MHz	517.25 [517.07]	489.50 [489.34]	475.91 [475.75]	512.35 [512.16]
q_2^J / kHz	-20.66 [-20.66]	-17.73 [-17.72]	-17.80 [-17.79]	-31.92 [-31.90]
q_2^{JJ} / Hz	1.485 [1.484]	1.205 [1.205]	1.189 [1.188]	3.024 [3.024]
q_2^{JJJ} / mHz	-0.151 [-0.150]	-0.118 [-0.118]	-0.112 [-0.112]	-0.375 [-0.378]
q_2^{JJJJ} / μHz	0.017 [0.016]	0.012 [0.013]	0.012 [0.011]	0.053 [0.056]
σ_q / Hz	1.28 [2.40]	2.67 [1.59]	2.32 [2.29]	1.74 [1.74]
α_2 / MHz	-194.31 [-194.30]	-160.79 [-160.80]	-179.81 [-179.81]	-324.73 [-324.61]
$B_2^{\rm est}$ / MHz	44938.37 [44938.23]	43465.99 [43466.54]	43055.73 [43056.17]	38517.92 [38517.78]
$B_2^{\rm exp}$ / MHz	44939.7878(38)[a]			
T_3 /cm^{-1}	1901.59 [1901.32]	1862.26 [1862.01]	1858.88 [1858.63]	1840.02 [1839.77]
B_3 / MHz	44166.72	42747.90	42327.67	37763.65
$B_3 - B_3^a$ / MHz	14.13	13.18	13.05	10.31
D_3 / kHz	115.47 [115.39]	107.37 [107.30]	105.47 [105.40]	94.06 [94.01]
H_3 / Hz	1.064 [1.066]	0.724 [0.725]	0.722 [0.722]	2.354 [2.352]
L_3 / mHz	-0.245 [-0.251]	-0.090 [-0.091]	-0.067 [-0.067]	-0.251 [-0.250]
K_3 /μHz	0.112 [0.119]	0.026 [0.026]	0.012 [0.012]	0.026 [0.023]
σ_3 / Hz	9.42 [8.36]	3.82 [6.08]	5.11 [5.39]	1.66 [5.76]
α_3 / MHz	358.34 [358.16]	343.68 [343.50]	337.60 [337.44]	260.70 [260.59]
$B_3^{\rm est}$ / MHz	44385.72 [44385.77]	42961.52 [42962.23]	42538.32 [42538.93]	37932.49 [37932.58]
T_1 /cm^{-1}	3277.34 [3276.54]	3263.63 [3262.83]	3276.86 [3276.06]	2483.25 [2482.93]
B_1 / MHz	44240.69	42835.12	42398.30	37728.43
$B_1 - B_1^a$ / MHz	14.21	13.27	13.13	10.30
D_1 / kHz	115.08 [115.01]	106.88 [106.81]	105.21 [105.14]	99.93 [99.88]
H_1 / Hz	1.046 [1.045]	0.820 [0.820]	0.840 [0.839]	3.434 [3.434]
L_1 / mHz	-0.068 [-0.067]	-0.058 [-0.058]	-0.053 [-0.053]	-0.421 [-0.425]
K_1 /μHz				0.056 [0.058]
σ_1 / Hz	15.13 [14.12]	13.43 [11.59]	6.71 [6.71]	2.13 [3.84]
α_1 / MHz	284.37 [284.27]	256.45 [256.37]	266.97 [266.89]	295.92 [295.80]
$B_1^{\rm est}$ / MHz	44459.69 [44459.65]	43048.75 [43049.36]	42608.95 [42609.48]	37897.27 [37897.37]
$B_1^{\rm exp}$ / MHz	44457.10(24)[c]			
${}^{(n)}B_e^{\rm est}[{}^{(a)}B_e^{\rm est}]$/ MHz	44786.69 [44786.50]	43370.40 [43370.86]	42920.21 [42920.59]	38046.09 [38046.18]
$S_0[S_0^a]$ /MHz	127.04 [126.91]	139.27 [139.13]	122.18 [122.01]	-46.42 [-46.41]
ΔB_0 / MHz	42.69 [42.57]	65.25 [65.13]	44.34 [44.23]	-147.04 [-146.99]
$\Delta B_0 - S_0$ / MHz	-84.35	-74.02	-77.84	-100.62

[a] Amano and Maeda.[17]
[b] calculated from the transition $J = 0 \rightarrow 1$ observed by Gudeman and Woods.[18,19]
[c] Nakanaga and Amano.[22]

lates a $B_0^{\rm exp}$ of 41 409.994 MHz. In Table VII on page 373 of his Ph.D. thesis,[14] Warner, however, reports a ground state rotational constant of 41 411.773 MHz for $H^{18}O^{13}C^+$. This result can be obtained from the observed rotational $J = 2 \rightarrow 3$ transition only under the assumption of $D_0^{\rm exp} = 98.83$ kHz. Interestingly, the latter $B_0^{\rm exp}$ and $D_0^{\rm exp}$ values agree nicely with our results of Table IV reported in Paper I, where $B_0^{\rm est} = 41\,411.39$ MHz and $D_0 = 96.64$ kHz are given for $H^{18}O^{13}C^+$.

A. Improving the equilibrium structure

The ground state vibrational correction ΔB_0 to the equilibrium rotational constant is derived from our calculations as

$$\Delta B_0 = B_e^{th} - B_0^{th}\,, \tag{2}$$

where B_e^{th} and B_0^{th} are theoretical values of the rotational constant at equilibrium and in the ground vibrational state, respectively. The equilibrium geometry used in Eq. (2) to evaluate B_e^{th} is the geometry corresponding to the minimum of the CCSD(T)/cc-pVQZ potential energy surface. Combining ΔB_0 of Eq. (2) with a ground-state rotational constant $B_0^{\rm exp}$ known from experiment, we may derive a new estimate of the equilibrium rotational constant $B_e^{\rm est}$ for a given isotopic species as

$$B_e^{\rm est} = B_0^{\rm exp} + \Delta B_0\,. \tag{3}$$

Knowing the experimental $B_0^{\rm exp}$ constant for several isotopologues, the values for $B_e^{\rm est}$ of Eq. (3) can be used to determine the equilibrium r_e molecular structure. The estimate $B_v^{\rm est}$ for the effective rotational constant in the vibrational state v is then

$$B_v^{\rm est} = B_e^{\rm est} - \Delta B_0 - \alpha_v\,, \tag{4}$$

where the vibration-rotation interaction constant α_v is

$$\alpha_v = B_0^{\rm th} - B_v^{\rm th} \qquad \text{for} \qquad v = 1 - 3\,. \tag{5}$$

For a linear triatomic molecule HXY, the equilibrium rotational constant B_e is expressed in terms of Jacobi coordinates r, R as

$$B_e = \frac{\hbar^2}{2\,I_e} = \frac{\hbar^2}{2\,(\mu_r\,r_e^2 + \mu_R\,R_e^2)}\,, \tag{6}$$

where the equilibrium distances r_e and R_e stand for

$$\begin{aligned} r_e &= r_e({\rm XY})\,, \\ R_e &= r_e({\rm HX}) + \frac{m_{\rm Y}}{m_{\rm XY}}\,r_e({\rm XY}) \end{aligned} \tag{7}$$

using $m_{\rm XY} = m_{\rm X} + m_{\rm Y}$. The reduced masses μ_r and μ_R are defined by

$$\mu_r = \frac{m_{\rm X}\,m_{\rm Y}}{m_{\rm XY}} \quad \text{and} \quad \mu_R = \frac{m_{\rm H}\,m_{\rm XY}}{m_{\rm HXY}}\,, \tag{8}$$

where $m_{\rm HXY} = M$ is the total molecular mass. The explicit values of μ_R, μ_r obtained using the atomic m_a and nuclear m_n masses are shown in Table I for the parent HCO^+ species. The atomic-mass values are larger by approximately 0.03-0.05 %, implying that the harmonic wavenumbers for the nuclear-mass case are larger by approximately 0.01-0.03 % (up to 1 $\rm cm^{-1}$).

The B_e value of a single isotopologue is clearly insufficient to uniquely determine r_e. The equilibrium structures of HCO^+ and HOC^+ are therefore extracted from a set of B_e values for several isotopologues by means of a Levenberg-Marquardt nonlinear least-squares algorithm[23] and using experimental uncertainties to compute weights. The analytical expression of Eq. (6) for the equilibrium rotational constant B_e was used in combination with analytical expressions for the partial derivatives of B_e with respect to the geometric parameters r_e(HX) and r_e(XY). The equilibrium bond lengths r_e(HX) and r_e(XY) calculated by this procedure for HCO^+ and HOC^+ are summarized in Table V, where we also show $r_e({\rm HY}) = r_e({\rm HX}) + r_e({\rm XY})$. The results of the calculations using atomic masses are taken from Paper I. Rows denoted by DBPC show the experimental r_e values for HCO^+ from the work of Dore and coworkers.[15] We were able to reproduce their r_e results, shown in Table XI of Ref. 15, by using B_e values from their Table X and atomic masses (row DBPC atomic).[24] Combining the B_e values of Dore et al. with nuclear masses, we calculated the nuclear-mass counterparts (row DBPC nuclear).

Upon substitution of the atomic masses of the constituent species with their nuclear counterparts, the length r_e(HX) of the bond involving hydrogen decreases by 1.8×10^{-4} Å for HCO^+ and by 7×10^{-5} Å for HOC^+,

TABLE V: Equilibrium distances (in Å) of HCO^+ and HOC^+ derived using nuclear and atomic masses. Fit U refers to results from an unweighted fit and DBPC refers to results based on Ref. 15. See Section II A for details.[a]

HCO^+	r_e(HC)	r_e(CO)	r_e(HO)
atomic masses	1.091 981(7)	1.105 615(2)	2.197 60(1)
nuclear masses	1.091 80(3)	1.105 874(9)	2.197 67(4)
Fit U atomic	1.092 00(1)	1.105 609(3)	2.197 61(2)
Fit U nuclear	1.091 87(5)	1.105 85(1)	2.197 72(6)
DBPC atomic	1.092 04	1.105 58	2.197 62
DBPC nuclear	1.091 93(3)	1.105 816(8)	2.197 75(4)
HOC^+	r_e(HO)	r_e(CO)	r_e(HC)
atomic masses	0.990 482(7)	1.154 468(2)	2.144 95(1)
nuclear masses	0.990 41(3)	1.154 692(7)	2.145 10(4)
Fit U atomic	0.990 50(2)	1.154 464(4)	2.144 96(2)
Fit U nuclear	0.990 46(7)	1.154 68(1)	2.145 13(7)

[a] Values in parentheses show one standard error to the last significant digits of the distances from the least-squares procedure.

whereas the equilibrium bond length r_e(CO) increases by 1.6×10^{-4} Å for HCO^+ and by 2.3×10^{-4} Å for HOC^+ in Table V. The overall length r_e(HY) of the cations is larger for the nuclear masses by approximately 1×10^{-4} Å. In other words, the effect of the substitution of the atomic masses with the nuclear masses is in order of 10^{-4} Å for the equilibrium bond lengths and is thus larger than accepted statistical uncertainties for r_e shown in Table V.

The equilibrium bond distances of Table V are used to calculate the equilibrium rotational constants, denoted by ${}^{(n)}B_e^{\rm est}$ and ${}^{(a)}B_e^{\rm est}$ in the nuclear-mass and atomic-mass case, respectively. The new estimates of the effective rotational constants $B_v^{\rm est}$ are derived for $v = 0-3$ by means of Eqs. (3) and (4). The values of $B_e^{\rm est}$ and $B_v^{\rm est}$ are listed in Tables II-IV. They both agree with their atomic-mass counterparts within 1.5 MHz for HCO^+ and within 0.5 MHz for HOC^+.

Our estimates r_e(HX), r_e(CO) of Table V reproduce the fitted $B_e^{\rm est}$ values with root-mean-square (rms) deviations of 0.8 [0.2] MHz for HCO^+ isotopologues and of 0.5 [0.2] MHz for HOC^+ isotopologues in the calculations using nuclear [atomic] masses, with a largest individual difference of 1.7 [0.4] MHz for $H^{13}C^{18}O^+$. In our fitting procedure, experimental data coming from different sources were employed, with experimental standard deviations for B_0^{exp} varying from 0.000 16 MHz (HCO^+) to 0.040 MHz ($HC^{18}O^+$) in the case of the HCO^+ cation. To test the sensititity of our results to these values, we also carried out unweighted nonlinear least-squares fits, denoted by Fit U in Table V. The equilibrium distances found in the original and Fit U differ by approximately 1×10^{-5} Å. This difference is thus comparable with statistical uncertainties of r_e within one to two standard deviations. In Fit U, the $B_e^{\rm est}$ values of HCO^+ isotopologues are reproduced with a rms deviation of 0.5 [0.1] MHz and a maximum individual deviation of 0.9 [0.3] MHz for $H^{13}C^{18}O^+$.

III. ROTATIONAL CONSTANTS AND THE DETERMINATION OF MOLECULAR STRUCTURE

The equilibrium geometry is the nuclear arrangement corresponding to the minimum of the potential energy surface for a given electronic state, computed in the framework of the Born-Oppenheimer approximation. The experimental counterpart is the r_e structure. This is a single geometric structure, which reproduces with high accuracy the experimental equilibrium constants derived by correcting the zero-point rotational constants for vibrational effects.[5] In the case of linear triatomic molecules, whose geometric arrangements are described by two bond distances, two isotopologues are required for the determination of the geometric parameters from the experimental (rotational) data. In real vibrating-rotating molecules (real experimental situation), the ground vibrational state is described by a wave function of some (sometimes also considerable) extent over close-to-equilibrium arrangements. Such a situation leads to an effective vibrationally averaged rotational constant B_0 different from the equilibrium B_e value. The zero-point rotational constants B_0 are experimentally available, but not B_e.

Two traditional approaches of experimental spectroscopy for the determination of the molecular structure are the r_0 approach (the r_0 structure), which directly uses the B_0 values, and the r_s approach (the substitution structure), which employs the analytical solutions of Kraitchman's equations.[4,25]

The so-called r_0 structure is computed from the zero-point rotational constants B_0. Whereas the equilibrium structure is well-defined and unique within the Born-Oppenheimer approximation, this is not the case with the concept of the r_0 geometry. To exemplify this issue, we provide the radial amplitude Δ_r for the ground vibrational state and several J values in Table VI. There the radial amplitude Δ_r is the difference between the expectation value of the coordinate $r = r(\mathrm{XY})$ in the rovibrational state $|n\rangle$ and the equilibrium distance $r_e = r_e(\mathrm{XY})$,

$$\Delta_r^{(n)} = \Delta_r = \langle n \mid r \mid n \rangle - r_e \,. \tag{9}$$

A quick glance at Table VI shows that Δ_r is isotopologue-dependent and J-dependent. The same also applies for the expectation values $\langle r \rangle$. For a given isotopic variant, Δ_r increases by approximately 5×10^{-4} Å for $J = 15$ with respect to the $J = 0$ result and decreases by approximately 5×10^{-4} Å with respect to the result for the parent molecule. In our rovibrational calculations, the expectation values $\langle r \rangle$ are found to be almost unaffected by the substitution of atomic masses by nuclear masses, such that Table VI applies to both the atomic-mass and nuclear-mass case.

In addition to the fact that the effective r_0 structural parameters are different for different isotopic forms, we may also remember that

$$\langle B \rangle = \left\langle \frac{\hbar^2}{2I} \right\rangle \neq \frac{\hbar^2}{2\,\langle I \rangle} = R_I \tag{10}$$

from a mathematical point of view. This is relevant for theoretical approaches. Whereas the integral $\langle I \rangle$ can be solved analytically, the integral $\langle B \rangle$ is solvable only by numerical means. To substantiate this issue, we compare in Table VII the ground state rotational constant B_0 with the vibrationally averaged value $\langle B \rangle$ and with R_I for HCO^+ and DCO^+. The values of R_I are computed using analytical integrals and the basis set expansion of the full-dimensional wavefunction for J=0. In Table VII, the quantity $B_{0\to1}$ is additionally shown, which is computed from the ground-state energies $E_0(J,p)$ as

$$B_{0\to1} = \tfrac{1}{2}\left[E_0(J=1,p=1) - E_0(J=0,p=0)\right] \,, \tag{11}$$

where p stands for parity. The results for B_0 are taken from Tables II and III, respectively.

TABLE VI: Amplitude Δ_r (in Å) in the ground vibrational state of the isotopic variants of HCO^+ and HOC^+ with the total rotational angular momentum $J = 0, 5, 10$, and 15.

HCO^+					HOC^+				
species	$J=0$	$J=5$	$J=10$	$J=15$	species	$J=0$	$J=5$	$J=10$	$J=15$
HCO^+	0.00469	0.00475	0.00490	0.00517	HOC^+	0.00853	0.00864	0.00885	0.00922
$HC^{17}O^+$	0.00464	0.00469	0.00485	0.00512	$H^{17}OC^+$	0.00848	0.00858	0.00880	0.00911
$HC^{18}O^+$	0.00459	0.00464	0.00480	0.00506	$H^{18}OC^+$	0.00842	0.00848	0.00869	0.00906
$H^{13}CO^+$	0.00453	0.00459	0.00475	0.00501	$HO^{13}C^+$	0.00842	0.00853	0.00874	0.00906
$H^{13}C^{17}O^+$	0.00459	0.00464	0.00480	0.00506	$H^{17}O^{13}C^+$	0.00837	0.00842	0.00864	0.00901
$H^{13}C^{18}O^+$	0.00448	0.00453	0.00469	0.00496	$H^{18}O^{13}C^+$	0.00832	0.00837	0.00858	0.00895
DCO^+	0.00453	0.00459	0.00469	0.00485	DOC^+	0.00795	0.00800	0.00816	0.00842
$DC^{17}O^+$	0.00448	0.00453	0.00464	0.00480	$D^{17}OC^+$	0.00784	0.00790	0.00811	0.00837
$DC^{18}O^+$	0.00443	0.00448	0.00459	0.00475	$D^{18}OC^+$	0.00779	0.00784	0.00800	0.00827
$D^{13}CO^+$	0.00443	0.00448	0.00459	0.00480	$DO^{13}C^+$	0.00784	0.00790	0.00805	0.00832
$D^{13}C^{17}O^+$	0.00438	0.00443	0.00453	0.00469	$D^{17}O^{13}C^+$	0.00774	0.00779	0.00795	0.00821
$D^{13}C^{18}O^+$	0.00432	0.00438	0.00448	0.00464	$D^{18}O^{13}C^+$	0.00768	0.00774	0.00790	0.00816

TABLE VII: Various representations of the ground state rotational constants computed for HCO^+ and DCO^+ using nuclear masses.

	B_0	$B_{0\to1}$	$\langle B\rangle$	R_I
HCO^+				
(MHz)	44391.37	44391.21	44245.40	44155.26
(cm^{-1})	1.48074	1.48073	1.47587	1.47286
DCO^+				
(MHz)	35861.59	35861.48	35743.61	35675.60
(cm^{-1})	1.19621	1.19621	1.19228	1.19001

For the vibrational ground state of HCO^+, the vibrationally averaged moments of inertia is 14.166 uÅ^2. Compared to B_0, the values for $\langle B\rangle$ and R_I are smaller by approximately 100 and 200 MHz, respectively, what amounts to 0.5 %. On the other hand, the value for $B_{0\to1}$, computed according to Eq. (11) from the ground state energies for $J = 0, 1$ only, differ by 0.16 and 0.11 MHz from the B_0 result for HCO^+ and DCO^+, respectively. This finding leads us to the conclusion that Coriolis coupling does not play an important role in the internal dynamics of both HCO^+ and DCO^+. The comparison of the values presented in Table VII also indicates that rovibrational calculations, carried out even for only a modest number of J values, may provide more useful results for B than their vibrationally averaged counterparts obtained from solely $J = 0$ computations.

The determination of structural parameters from the experimental data is very often carried out by the employment of the moments of inertia, which are reciprocals of the rotational constants, Eq. (6). The positions z_1, z_2, z_3 of the aligned atoms H, X, Y in the reference system with the origin in the center of mass of the parent molecule HXY are explicitly

$$\begin{aligned} M\,z_1 &= -m_{\rm XY}\,x - m_{\rm Y}\,y\,,\\ M\,z_2 &= m_{\rm H}\,x - m_{\rm Y}\,y\,,\\ M\,z_3 &= m_{\rm H}\,x + m_{\rm HX}\,y\,, \end{aligned} \tag{12}$$

where $x = r(\mathrm{HX})$ and $y = r(\mathrm{XY})$. The difference ΔI between the moments of inertia of two different isotopic forms is then

$$\begin{aligned} \Delta I = I_2 - I_1 =& (a_2 - a_1)\,x^2 \\ &+ (b_2 - b_1)\,x\,y + (c_2 - c_1)\,y^2\,. \end{aligned} \tag{13}$$

For explicit values of the parameters a_i, b_i, c_i, see Eq. (A4) of the Appendix. It is an easy matter to derive for a simple substitution $m_i \to m_i'$ and $i = 1 - 3$ that

$$\begin{aligned} \Delta I(m_{\rm H}\to m'_{\rm H}) =& \frac{m'_{\rm H} - m_{\rm H}}{M\,M'}\,(m_{\rm XY}\,x + m_{\rm Y}\,y)^2\,,\\ \Delta I(m_{\rm X}\to m'_{\rm X}) =& \frac{m'_{\rm X} - m_{\rm X}}{M\,M'}\,(m_{\rm H}\,x - m_{\rm Y}\,y)^2\,,\\ \Delta I(m_{\rm Y}\to m'_{\rm Y}) =& \frac{m'_{\rm Y} - m_{\rm Y}}{M\,M'}\,(m_{\rm H}\,x + m_{\rm HY}\,y)^2\,, \end{aligned} \tag{14}$$

implying

$$z_i^2 = \frac{M'}{M\,(m'_{\rm i} - m_{\rm i})}\,\Delta I(m_{\rm i}\to m'_{\rm i})\,. \tag{15}$$

The latter equation is known as Kraitchman's relation for linear triatomic molecules.[4] It provides the position

z_i of the ith atom with respect to the center of mass of the parent molecule as a function of the moment-of-inertia difference $\Delta I(m_{\rm i} \to m'_{\rm i})$. From three known z_1, z_2, z_3 values, the bond distances are calculated as $r(\mathrm{HX}) = x = z_2 - z_1$ and $r(\mathrm{XY}) = y = z_3 - z_2$. To compute two distances of a linear triatomic molecule by means of Eq. (15), we effectively need four B values available for the parent molecules HXY and three singly substituted species DXY, HX'Y, and HXY'.

Kraitchman's equation of Eq. (15) is frequently used for the estimation of the experimental equilibrium structure. Letting I_1 and I_2 be the moment of inertia of the parent molecule and of the substituted species, respectively, where

$$I_i = I_i^{(0)} = \frac{\hbar^2}{2\,B_0^{(i)}} \quad \text{for} \quad i = 1, 2\,, \tag{16}$$

then

$$\begin{aligned} \Delta I^{(0)} =& I_1^{(0)} - I_2^{(0)} = I_1^{(e)} - I_2^{(e)} + D_I \\ =& \Delta I^{(e)} + D_I = \Delta I\,. \end{aligned} \tag{17}$$

In the case that the vibrational corrections for two isotopic species in the ground vibrational state are similar, the deviation D_I in Eq. (17) will be small, so that $\Delta I^{(0)} \approx \Delta I^{(e)}$, implying that $\Delta I^{(0)}$ may be used instead of $\Delta I^{(e)}$. The structure obtained in this fashion is known as the substituted r_s structure. Only under the condition of $\Delta I^{(0)} \approx \Delta I^{(e)}$, the r_s structure will be a good approximation of the r_e structure. The r_m structure introduced by Watson, derived by approximating the equilibrium moment of inertia with $2I_s - I_0$, is found less satisfactory for hydrogen containing species,[5] where I_s is the moment of inertia computed using the r_s geometry.

Since two bond lengths of a linear triatomic molecule can be always determined from two moments of inertia available for two different isotopologues, we finally also examine a pair determination of the molecular structure. An analytic solution for the corresponding mathematical problem is provided in the Appendix. In the case when experimental data are known for n isotopic species, we can pair them in $N = n(n-1)/2$ different ways, yielding N pair solutions (x_i, y_i), where $x = r(\mathrm{HX})$ and $y = r(\mathrm{XY})$ for $i = 1, \ldots, N$. The mean pair values are

$$x^{\rm ap} = \frac{1}{N}\sum_{i=1}^{N} x_i \quad \text{and} \quad y^{\rm ap} = \frac{1}{N}\sum_{i=1}^{N} y_i\,. \tag{18}$$

To quantify the spread of the pair solutions (x_i, y_i) around the mean value $(x^{\rm ap}, y^{\rm ap})$, we introduce the average radius of the pair distribution $d_{\rm ap}$ as

$$d_{\rm ap} = \sqrt{\sum_{i=1}^{N} \frac{1}{N}\left[(x_i - x_1^{\rm ap})^2 + (y_i - y_2^{\rm ap})^2\right]}\,. \tag{19}$$

We will call the solution $(x^{\rm ap}, y^{\rm ap})$ a $r_{\rm ap}$ structure.

To correct for the rovibrational effects in B_0, one needs the effective rotational constants for the singly excited vibrational states and two isotopic forms in experimental spectroscopy. Knowing the effective rotational constants B_1, B_2, B_3, one may derive the vibration-rotation interaction constants $\alpha_1, \alpha_2, \alpha_3$, yielding the spectroscopic zero-point vibrational correction as

$$S_0 = \tfrac{1}{2}\,(\alpha_1 + 2\,\alpha_2 + \alpha_3) \tag{20}$$

for linear triatomic molecules in the traditional spectroscopic approach. Therefrom the experimental equilibrium rotational constant follows as

$${}^{(\alpha)}B_e^{\rm exp} = B_0^{\rm exp} + S_0\,. \tag{21}$$

We will denote by r_α the equilibrium structure derived from ${}^{(\alpha)}B_e^{\rm exp}$. In electronic-structure program packages, the expression of Eq. (21) has become a standard tool to compute the zero-point rotational constant B_0 from the calculated equilibrium geometry (providing B_e) and the zero-point vibrational correction S_0 computed according to Eq. (20) by means of second order vibrational perturbation theory.[26] This spectroscopic model is effectively based on the harmonic-oscillator-rigid-rotor description as a zero-order picture.

In our approach used here and in Paper I, the ground state vibrational corrections ΔB_0 are computed according to Eq. (2) as a difference between the rotational constant B_e^{th} at equilibrium of the CCSD(T)/cc-pVQZ potential energy surface and the rotational constant B_0^{th} in the ground vibrational state. The B_0^{th} values are derived from rovibrational energies computed for $J = 0-15$ by a numerically exact full-dimensional quantum-mechanical method. In addition to ΔB_0, we also derived the vibration-rotation interaction constants $\alpha_v = B_0^{th} - B_v^{th}$ of Eq. (5) and used them to calculate the spectroscopic correction S_0 according to Eq. (20). The quantities ΔB_0 and S_0 are both shown in Tables II-IV. The difference between ΔB_0 and S_0 is in order of 1 MHz for the hydrogen containing forms of HCO^+ in Table II. However, $\Delta B_0 - S_0$ is as large as 50 and 100 MHz for DCO^+ and DOC^+ in Tables III and IV, respectively. In our calculations, the mass effect on ΔB_0 and S_0 is smaller than 0.2 MHz.

A. Results

In the case when experimental data are available for a series of isotopic variants, the determination of the geometric parameters may proceed employing different mathematical procedures. Nonlinear fitting algorithms are expected to give the best over-all fit to all of the rotational constants. Analytical solutions using Kraitchman's relations are applicable for the parent molecule and three singly substituted species. The geometry problem can be also solved analytically for any pair of isotopic variants. The rotational constants not included in the

TABLE VIII: Structural parameters (in Å) obtained for HCO^+ and HOC^+ by means of Kraitchman's relations. Root-mean-square (rms) deviations are in MHz. Values shown in brackets for HCO^+ are rms deviations for the rotational constants of all eight isotopologues.

HCO^+							
source	structure	atomic mass			nuclear mass		
		r(HC)	r(CO)	rms	r(HC)	r(CO)	rms
$B_0^{\rm exp}$	$r_s^{(0)}$	1.092 921	1.107 228	108.1 [101.3]	1.092 926	1.107 236	121.2 [113.5]
$B_0^{\rm exp} + S_0$	$r_s^{(\alpha)}$	1.098 720	1.104 852	32.5 [46.5]	1.098 732	1.104 862	19.8 [37.1]
$B_0^{\rm exp} + \Delta B_0$	$r_s^{(e)}$	1.092 014	1.105 560	2.9 [2.7]	1.092 020	1.105 568	15.8 [14.8]
HOC^+							
source	structure	atomic mass			nuclear mass		
		r(HO)	r(CO)	rms	r(HO)	r(CO)	rms
$B_0^{\rm exp}$	$r_s^{(0)}$	0.964 099	1.159 471	7.5	0.964 102	1.159 478	18.4
$B_0^{\rm exp} + S_0$	$r_s^{(\alpha)}$	0.984 741	1.155 069	52.8	0.984 759	1.155 071	40.2
$B_0^{\rm exp} + \Delta B_0$	$r_s^{(e)}$	0.990 522	1.154 383	4.8	0.990 543	1.154 387	17.3

process of determining the geometry by analytical means will generally be less well predicted, such that the resulting structure will be a less balanced representation compared to the structure from the nonlinear fits of all available isotopologues.

A more serious obstacle to the derivation of an equilibrium structure is related to uncertainties which occur as a necessary consequence of the effects due to zero-point vibrations. We investigated this issue in practical terms by considering the ground state vibrational corrections given as ΔB_0 of Eq. (2) and as S_0 of Eq. (20).

The structural parameters of HCO^+ and HOC^+ derived in different approaches are summarized in Tables VIII and IX. The results are presented for both the atomic-mass and nuclear-mass cases. The root-mean-square (rms) deviation is employed as a measure of goodness of the derived bond lengths to predict the corresponding set of rotational constants. Eight isotopic variants of HCO^+ and four of HOC^+ are considered.

Table VIII summarizes distances derived using Kraitchman's relations. The main isotopic forms of HCO^+ and HOC^+ were chosen as parent species. The four isotopic variants considered, for instance, for the formyl cation were HCO^+, DCO^+, $H^{13}CO^+$, and $HC^{18}O^+$. Three sets of data are studied using the experimental zero-point rotational constants $B_0^{\rm exp}$ shown in Tables II-IV. The values of $B_0^{\rm exp}$ uncorrected for vibrational effects form the first set, yielding the substitution structure denoted by $r_s^{(0)}$ in Table VIII. The second set composed of $B_0^{\rm exp} + S_0$ produces the $r_s^{(\alpha)}$ structure, whereas the third set based on the values of $B_0^{\rm exp} + \Delta B_0$ gives the $r_s^{(e)}$ structure. For ΔB_0 and S_0, we use our theoretical values. Note that the structure $r_s^{(0)}$ is commonly called the r_s structure in the spectroscopic literature.

The distances in Table VIII show negligible variations upon the replacement of atomic masses with their nuclear counterparts. This is to be expected from the mathematical form of Kraitchman's relation in Eq. (15), which involves explicit mass dependence only through the factor $f_m = M'/M\,(m_{\rm i}' - m_{\rm i})$. The difference between the f_m values computed using atomic and nuclear masses is somewhat smaller than $1 \times 10^{-5}\,{\rm u}^{-1}$ for the studied systems. To facilitate comparison between distances obtained using the atomic and nuclear masses, the values in Table VIII are given with six decimal places.

The r_s distances in Table VIII exhibit a broad spread of 0.006 and 0.026 Å for HCO^+ and HOC^+, respectively. The large difference of approximately 6-7$\times 10^{-3}$ Å between the $r_s^{(\alpha)}$(HX) and $r_s^{(e)}$(HX) distances arises from a large difference of 54 and 100 MHz between the S_0 and ΔB_0 values for DCO^+ and DOC^+ in Tables III and IV, respectively. Compared to the equilibrium distances of Table V, the $r_s^{(e)}$(HX) bond length is longer by $3 - 4 \times 10^{-5}$ Å and $r_s^{(e)}$(XY) shorter by $4 - 8 \times 10^{-5}$ Å in the atomic-mass case. These differences are in order of 10^{-4} Å for the nuclear-mass case since the r_s distances are nearly insensitive to the replacement of atomic masses with their nuclear counterparts.

For given r_s distances, rotational constants for all isotopologues were evaluated according to Eq. (6). The rms deviations in Table VIII are thus a measure of goodness of the approximation of the equilibrium rotational constant by $B_0^{\rm exp}$, $B_0^{\rm exp} + S_0$, and $B_0^{\rm exp} + \Delta B_0$ in the case of the $r_s^{(0)}$, $r_s^{(\alpha)}$, and $r_s^{(e)}$ structure, respectively. Among

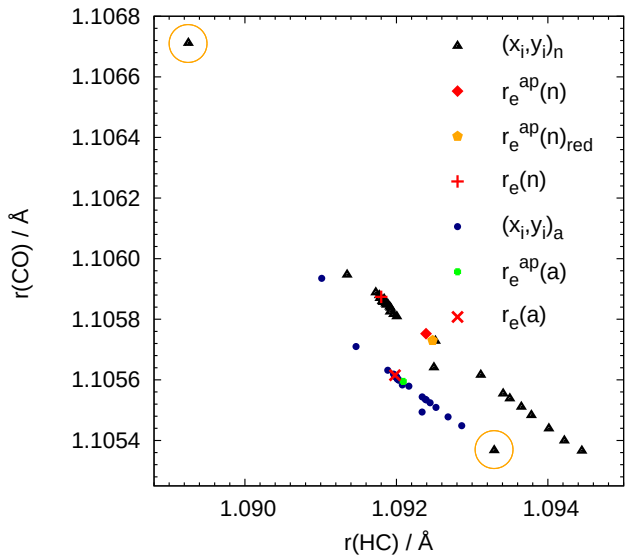

FIG. 1: Pair solutions $(x_i, y_i)_a$ and $(x_i, y_i)_n$ for HCO^+ obtained for the atomic and nuclear masses, respectively, from $B_0^{\rm exp} + \Delta B_0$. Explicit values of r_e(a), $r_e^{\rm ap}$(a) for the atomic masses and r_e(n), $r_e^{\rm ap}$(n) for the nuclear masses are found in Table IX. For the definition of $r_e^{\rm ap}(n)_{\rm red}$, see the main text.

the three representations in Table VIII, the $r_s^{(e)}$ distances perform the best, providing the smallest rms deviation. Root-mean-square deviations are somewhat larger for the nuclear-mass case than for the atomic-mass case.

The three sets of data involving the $B_0^{\rm exp}$, $B_0^{\rm exp} + S_0$, and $B_0^{\rm exp} + \Delta B_0$ values are now used in combination with a nonlinear least-squares procedure, yielding the r_0, r_α, and r_e distances, respectively. These results are summarized in Table IX. In Fit 4 there, we employ the data for the four HCO^+ isotopologues used to derive Kraitchman's solutions of Table VIII. The r_e distances of Table V are repeated in bold face in Table IX. For the r_0 and r_e structures, we also give the mean pair solutions of Eq. (18), denoted by $r_0^{\rm ap}$ and $r_e^{\rm ap}$, respectively. The mean radius of the pair distribution is defined by Eq. (19). Inspired by the approach of Kraitchman, we also tested a fitting procedure for the differences of rotational constants. These results are labelled with $r_0^{\rm diff}$ and $r_e^{\rm diff}$. In addition to the rms deviations for the rotational constants, Table IX also shows rms errors for the differences of the rotational constants in brackets. For our data sets, the total number of pairs and differences is 28 for HCO^+ and 6 for HOC^+.

All of the pair solutions for $B_0^{\rm exp} + \Delta B_0$ of HCO^+ are graphically displayed in Fig. 1. The pair solutions derived in the atomic-mass case lie in $x_i \in (1.0910\,\mathring{A}, 1.0929\,\mathring{A})$ and $y_i \in (1.1054\,\mathring{A}, 1.1059\,\mathring{A})$. The pair solutions obtained using nuclear masses are distributed over a larger space, occupying $x_i \in (1.0892\,\mathring{A}, 1.0944\,\mathring{A})$ and $y_i \in (1.1054\,\mathring{A}, 1.1067\,\mathring{A})$. Most of the solutions are aligned or nearly aligned for both the atomic-mass and nuclear-mass cases in Fig. 1. Two $(x_i, y_i)_n$ pairs for the nuclear masses falling out of line are circled in Fig. 1. Eliminating them from the averaging process, the mean value $(x_e^{\rm ap}, y_e^{\rm ap})$ is changed from $(1.09239\,\mathring{A}, 1.10575\,\mathring{A})$ to a value of $(1.09213\,\mathring{A}, 1.10558\,\mathring{A})$. This solution is denoted by $r_e^{\rm ap}(n)_{\rm red}$ in Fig. 1.

The estimates r_e for the equilibrium bond distances reproduce the rotational constants $B_0^{\rm exp} + \Delta B_0$ with a rms deviation of about 0.2 [0.8] MHz in the atomic-mass [nuclear-mass] case, as seen in Table IX. This implies that $B_0^{\rm exp} + \Delta B_0$ approximates fairly well the equilibrium rotational constant $B_e^{\rm exp}$. Rms deviations of approximately 5 MHz are seen for the r_0 parameters, which are computed from $B_0^{\rm exp}$. In the case of the r_α structure, the results for $B_0^{\rm exp} + S_0$ are reproduced by the linear-molecule model of Eq. (6) with rms deviations of about 20 MHz for HCO^+ and 2 MHz for HOC^+.

The three r_0, r_α, r_e geometries in Table IX are different. For HCO^+, the distance r_0(HC) is shorter by 0.0006 Å and r_α(HC) longer by 0.004 Å than r_e(HC), whereas r_0(CO) is longer by 0.004 Å and r_α(CO) shorter by 0.0008 Å than r_e(CO). In the case of HOC^+, the r_α geometry deviates somewhat less than the r_0 geometry from the r_e results. Interestingly, the pair solution $r_e^{\rm ap}$ and the solution $r_e^{\rm diff}$, obtained by fitting the differences of the rotational constants, agree with each other within $1-2\times10^{-5}$ Å. They both, however, differ by $1\text{-}2\times10^{-4}$ Å from the r_e structure.

Another salient feature is observed by comparing the results for r_0, r_α, r_e from Fit 4 of Table IX with the values of $r_s^{(0)}, r_s^{(\alpha)}, r_s^{(e)}$ derived from Kraitchman's relations in Table VIII. In all three cases, rms deviations are smaller for the geometric parameters obtained by nonlinear least-squares fits, which thus appear more appropriate for the determination of molecular structures.

IV. FINAL REMARKS

Accurate determination of the equilibrium geometry of molecules is considered as one of the most important goals of spectroscopy. Geometric parameters are unambiguously determined only from actual equilibrium rotational constants B_e, which, however, are not accessible experimentally. Experimental spectroscopy thus takes on other views of the situation. If there is no data on excited vibrational states, two traditional approaches to determining the molecular structure are the r_0 approach, which uses the zero-point rotational constants B_0 directly, and the r_s approach, which uses Kraitchman's relations in combination with B_0. In the case when information is available on singly excited vibrational states, the zero-point rotational constants B_0 are corrected for the vibrational effects with the help of the spectroscopic correction S_0 of Eq. (20) to give ${}^{(\alpha)}B_e^{\rm exp}$ of Eq. (21), yielding the r_α structure. The three sets r_0, r_s, r_α of geometric parameters are generally different. Modifications of data sets, such as a change of a parent molecule in the Kraitchman's approach, may introduce additional inconsisten-

TABLE IX: Various structural parameters (in Å) obtained for HCO^+ and HOC^+ by means of a nonlinear least-squares technique. Root-mean-square (rms) deviations are shown in MHz. For more details, see the main text.[a]

HCO^+								
structure	atomic mass				nuclear mass			
	r(HC)	r(CO)	rms	$d_{\rm ap}$	r(HC)	r(CO)	rms	$d_{\rm ap}$
r_0	1.091 42(22)	1.109 32(6)	5.0 [5.7]		1.091 23(24)	1.109 59(7)	5.6 [6.4]	
r_0 (Fit 4)	1.091 72(5)	1.109 27(1)	3.9 [4.5]		1.091 56(6)	1.109 52(2)	4.3 [5.0]	
$r_0^{\rm ap}$	1.095 47	1.108 46	15.1 [19]	7.1×10^{-3}	1.095 77	1.108 62	16.9 [21]	7.8×10^{-3}
$r_0^{\rm diff}$	1.095 30(10)	1.109 92(2)	92 [1.8]		1.095 54(11)	1.110 25(2)	102 [2.1]	
r_α	1.096 1(30)	1.104 8(9)	20.4 [31]		1.095 9(30)	1.105 1(9)	20.5 [31]	
r_α (Fit 4)	1.099 29(2)	1.104 197(7)	1.2 [1.6]		1.099 15(2)	1.104 449(5)	0.9 [1.2]	
$\mathbf{r_e}$	**1.091 981(7)**	**1.105 615(2)**	0.2 [0.2]		**1.091 80(3)**	**1.105 874(9)**	0.8 [0.9]	
r_e (Fit 4)	1.091 989(1)	1.105 614(3)	0.1 [0.1]		1.091 839(8)	1.105 867(2)	0.6 [0.7]	
$r_e^{\rm ap}$	1.092 09	1.105 59	0.5 [0.5]	3.5×10^{-4}	1.092 39	1.105 75	2.4 [2.7]	1.1×10^{-3}
$r_e^{\rm diff}$	1.092 104(7)	1.105 634(1)	2.9 [0.1]		1.092 34(1)	1.105 957(2)	13 [0.4]	
HOC^+								
structure	atomic mass				nuclear mass			
	r(HO)	r(CO)	rms	$d_{\rm ap}$	r(HO)	r(CO)	rms	$d_{\rm ap}$
r_0	0.965 32(20)	1.159 31(5)	4.5 [7.1]		0.965 23(21)	1.159 53(6)	4.4 [7.0]	
$r_0^{\rm ap}$	0.959 80	1.160 18	21 [28]	0.016	0.960 24	1.160 32	19 [26]	0.017
$r_0^{\rm diff}$	0.968 0(12)	1.160 2(4)	87 [10]		0.968 3(12)	1.160 5(4)	99 [10]	
r_α	0.985 48(6)	1.154 07(2)	2.3 [3.1]		0.985 40(4)	1.154 30(1)	2.0 [2.7]	
$\mathbf{r_e}$	**0.990 482(7)**	**1.154 468(2)**	0.14 [0.18]		**0.990 41(3)**	**1.154 692(7)**	0.5 [0.6]	
$r_e^{\rm ap}$	0.990 69	1.154 43	0.7 [1.1]	2.5×10^{-4}	0.991 14	1.154 56	2.5 [3.6]	9.1×10^{-4}
$r_e^{\rm diff}$	0.990 62	1.154 51	4.5 [0.06]		0.990 92	1.154 85	16 [0.1]	

[a] Values in parentheses show one standard error to the last significant digits of the distances from the least-squares procedure.

cies among the values predicted by a chosen method.[14]

The concepts of the equilibrium geometry and the vibrational correction to the zero-point rotational constant are well founded in theoretical approaches, such that theory may provide useful assistance to experiment in the evaluation of the equilibrium structure. To achieve as accurate as possible corrections to B_e in the real situation of a vibrating and rotating molecule, theoretical methods for numerically exact quantum-mechanical calculations are desirable since only then we can have a proper full-dimensional physical answer for a given potential energy surface in the Born-Oppenheimer approximation. In the present work and previously in Paper I, we point to the difference between the spectroscopic correction S_0 of Eq. (20) and the zero-point correction ΔB_0, defined in Eq. (2) literally as a difference between the rotational constant at equilibrium and the rotational constant in the ground vibrational state. In connection with this, we also observed that rovibrational calculations, carried out even for lowest J values, may provide useful values of B_0. Unlike variational methods, vibrational second-order perturbational approaches are capable of providing only the spectroscopic correction S_0, which is not always sufficient to evaluate the molecular structure. The concept of the r_e structure is generally useful. Its applicability in the case of quasi-linear molecules and weakly bonded complexes deserves, however, some attention.

Another issue relevant for the determination of molecular geometries is related to the answer on the question 'which masses are vibrating or rotating in a molecule?', to cite the title of a paper by Kutzelnigg.[6] This question appears natural in connection with charged molecular systems, like HCO^+ and HOC^+, which lack an electron.

Several choices of mass are commonly used in nuclear dynamics computations. The atomic masses have became standard in connection with the Born-Oppenheimer approximation because the atomic masses are expected to minimize the deviation of the employed electronic-structure approach with respect to complete theory. For the Born-Oppenheimer approximation plus

adiabatic contributions, the nuclear masses are considered more adequate physically. Rescaled masses or distance-dependent masses are also encountered in some applications.[6,27,28] Systematic improvements of the computational approaches are possible only in conjunction with the nuclear masses.

In experimental studies, the atomic masses are tacitly in use,[5] so that an explicit reference regarding the employed masses is rarely given. In the case of HCO^+, we may note that Bogey et al.[12] made use of the atomic masses. In addition to the atomic masses, Warner[14] also performed several tests aiming at electron mass corrections in the framework of the r_s structure.

In the present work, we found that the replacement of the atomic masses with the nuclear masses affects the equilibrium bond lengths in order of 10^{-4} Å. This effect is larger than the accepted statistical uncertainties of 10^{-5} Å for the r_e parameters, such that the mass issue deserves some attention in molecular studies. We, however, also observed that the equilibrium structure obtained by the employment of the atomic masses is statistically somewhat better than the nuclear-mass counterpart. Regarding concrete mathematical approaches to solve for the equilibrium structure, a nonlinear fit of all available data is recommened as more trustworthy than other possible variants.

Dedication

This work is dedicated to William Klemperer. In 1970, Klemperer proposed the assignment of the X-ogen transition to HCO^+, leading to the identification of this species as the first cation in the interstellar environment and marking the beginning of the fascinating field of interstellar chemistry.

* Corresponding author; Electronic address: Mirjana.Mladenovic@u-pem.fr
† Electronic address: Marius.Lewerenz@u-pem.fr

[1] M. Mladenović, *J. Chem. Phys.* **147**, 114111 (2017).
[2] M. Mladenović and S. Schmatz, *J. Chem. Phys.* **109**, 4456 (1998).
[3] J. H. Van Vleck, *J. Chem. Phys.* **4**, 327 (1936).
[4] J. Kraitchman, *Amer. J. Phys.* **21**, 17 (1953).
[5] J. K. Watson, *J. Mol. Spectrosc.* **48**, 479 (1973).
[6] W. Kutzelnigg, *Mol. Phys.* **105**, 2627 (2007).
[7] B. Sutcliffe and R. G. Woolley, The Potential Energy Surface in Molecular Quantum Mechanics, in *Advances in Quantum Methods and Applications in Chemistry, Physics, and Biology. Progress in Theoretical Chemistry and Physics*, edited by M. Hotokka, E. Brändas, J. Maruani, and G. Delgado-Barrio, volume 27, pp. 3–40, Springer International Publishing, 2013.
[8] B. Sutcliffe and R. G. Woolley, The Position of the Clamped Nuclei Electronic Hamiltonian in Quantum Mechanics, in *Handbook of Computational Chemistry*, edited by J. Leszczynski, A. Kaczmarek-Kedziera, T. Puzyn, M. G. Papadopoulos, H. Reis, and M. K. Shukla, pp. 69–121, Springer International Publishing, 2017.
[9] I. Mills, T. Cvitaš, K. Homann, N. Kallay, and K. Kuchitsu, *Quantities, Units and Symbols in Physical Chemistry, Second Edition*, Blackwell Scientific Publications, Oxford, 1993.
[10] G. Cazzoli, L. Cludi, G. Buffa, and C. Puzzarini, *Astrophys. J. Suppl. Ser.* **293**, 1 (2012).
[11] L. Dore, C. Puzzarini, and G. Cazzoli, *Can. J. Phys.* **79**, 359 (2001).
[12] M. Bogey, C. Demuynck, and J. Destombes, *Mol. Phys.* **43**, 1043 (1981).
[13] V. Lattanzi, A. Walters, B. J. Drouin, and J. C. Pearson, *Astrophys. J.* **662**, 771 (2007).
[14] H. E. Warner, *The Microwave Spectroscopy of Ions and Other Transient Species in DC Glow and Extended Negative Glow Discharges*, Ph.D. thesis, University of Wisconsin-Madison, 1988.
[15] L. Dore, S. Beninati, C. Puzzarini, and G. Cazzoli, *J. Chem. Phys.* **118**, 7857 (2003).
[16] P. Caselli and L. Dore, *Astron. Astrophys.* **433**, 1145 (2005).
[17] T. Amano and A. Maeda, *J. Mol. Spectrosc.* **203**, 140 (2000).
[18] C. S. Gudeman and R. C. Woods, *Phys. Rev. Lett.* **48**, 1344 (1982).
[19] C. S. Gudeman and R. C. Woods, *Phys. Rev. Lett.* **48**, 1768 (1982).
[20] C. F. Neese, P. S. Kreynin, and T. Oka, *J. Phys. Chem. A* **117**, 9899 (2013).
[21] T. Hirao, S. Yu, and T. Amano, *J. Chem. Phys.* **127**, 074301 (2007).
[22] T. Nakanaga and T. Amano, *J. Mol. Spectrosc.* **121**, 502 (1987).
[23] W. H. Press, B. P. Flannery, S. A. Teukolsky, and W. T. Vetterling, *Numerical Recipes*, Cambridge University Press, Cambridge, 1986.
[24] Note a misprint in Table X of Ref.[15], where $B_e(HC^{18}O^+)$ should have a value of 42 811.0181(16) MHz.
[25] C. C. Costain, *J. Chem. Phys.* **29**, 864 (1958).
[26] C. Puzzarini, J. F. Stanton, and J. Gauss, *Int. Rev. Phys. Chem.* **29**, 273 (2010).
[27] R. Röhse, W. Kutzelnigg, R. Jaquet, and W. Klopper, *J. Chem. Phys.* **101**, 2231 (1994).
[28] R. Jaquet and M. V. Khoma, *J. Phys. Chem. A* **121**, 7016 (2017).

APPENDIX A: ANALYTICAL SOLUTION FOR BOND LENGTHS FROM TWO KNOWN MOMENTS OF INERTIA FOR THE CASE OF LINEAR TRIATOMIC MOLECULES

For linear triatomic molecules HXY, the equilibrium moment of inertia is explicitly

$$I_e = \mu_r\, r_e^2 + \mu_R\, R_e^2\,, \tag{A1}$$

where the bond lengths r_e, R_e are given by Eq. (7) and the reduced masses μ_r, μ_R by Eq. (8). Letting $x = r_e(\mathrm{HX})$ and $y = r_e(\mathrm{XY})$, Eq. (A1) is rewritten to

$$\begin{aligned} I_e =& \mu_r\, x^2 + \mu_R \left[x + \frac{m_\mathrm{Y}}{m_\mathrm{XY}}\, y\right]^2 \\ =& \frac{m_\mathrm{H}\, m_\mathrm{XY}}{M}\, x^2 + 2\,\frac{m_\mathrm{H}\, m_\mathrm{Y}}{M}\, x\, y + \frac{m_\mathrm{Y}\, m_\mathrm{HX}}{M}\, y^2\,, \end{aligned} \tag{A2}$$

in fact

$$I = a\, x^2 + b\, x\, y + c\, y^2\,, \tag{A3}$$

using

$$a = \frac{m_\mathrm{H}\, m_\mathrm{XY}}{M}\,, \quad b = 2\,\frac{m_\mathrm{H}\, m_\mathrm{Y}}{M}\,, \quad c = \frac{m_\mathrm{Y}\, m_\mathrm{HX}}{M}\,, \tag{A4}$$

and $M = m_\mathrm{H} + m_\mathrm{X} + m_\mathrm{Y}$.

The moment of inertia is the reciprocal of the rotational constant, Eq. (6). Knowing B_e for two different isotopic forms of a linear triatomic molecule, two values $I_e^{(1)}$ and $I_e^{(2)}$ become available. The equilibrium distances x and y can then be calculated by solving the following system of equations

$$\begin{aligned} d_1 =& a_1\, x^2 + b_1\, x\, y + c_1\, y^2\,, \\ d_2 =& a_2\, x^2 + b_2\, x\, y + c_2\, y^2\,, \end{aligned} \tag{A5}$$

where $d_1 = I_e^{(1)}$ and $d_2 = I_e^{(2)}$. Multiplying the first equation by b_2 and substracting the second equation multiplied by b_1, we obtain

$$(a_1\, b_2 - a_2\, b_1)\, x^2 = d_1\, b_2 - d_2\, b_1 + (b_1\, c_2 - b_2\, c_1)\, y^2\,. \tag{A6}$$

Substituting into Eq. (A5), we find that

$$\begin{aligned} (a_1\, b_2 - a_2\, b_1)\, x\, y =& a_1\, d_2 - a_2\, d_1 \\ & - (a_1\, c_2 - a_2\, c_1)\, y^2\,. \end{aligned} \tag{A7}$$

We square both sides of the equation and use Eq. (A6) to replace x^2, yielding

$$A\, y^4 + B\, y^2 + C = 0\,, \tag{A8}$$

where

$$\begin{aligned} A =& (a_1\, b_2 - a_2\, b_1)(b_2\, c_1 - b_1\, c_2) + (a_1\, c_2 - a_2\, c_1)^2\,, \\ B =& (b_1\, d_2 - b_2\, d_1)(a_1\, b_2 - a_2\, b_1) \\ & + 2(a_1\, d_2 - a_2\, d_1)(a_2\, c_1 - a_1\, c_2)\,, \\ C =& (a_1\, d_2 - a_2\, d_1)^2\,. \end{aligned} \tag{A9}$$

The two solutions for y^2 are thus

$$y_{1/2}^2 = \frac{-B \pm \sqrt{D}}{2A} \tag{A10}$$

with the determinant $D = B^2 - 4\,A\,C$ given explicitly by

$$\begin{aligned} D \;=\; & (a_1\, b_2 - a_2\, b_1)^2 \left[(b_1\, d_2 - b_2\, d_1)^2 \right. \\ & \left. + 4(a_1\, d_2 - a_2\, d_1)(c_1\, d_2 - c_2\, d_1)\right]\,. \end{aligned} \tag{A11}$$

The two solutions of Eq. (A10) for y^2 provide two results for y, taken as positive square roots since y is a distance. For each possible y, we use Eq. (A6) to determine x as a positive square root of x^2. The procedure may thus lead to two different solution pairs (x, y). This is a consequence of the squaring of Eq. (A7), which may introduce new solutions. Direct substitution in Eq. (A5) should be used to verify which of the two pairs is appropriate as a solution. In the case that both solutions are eligible with respect to Eq. (A5), additional criteria are needed. For instance, resulting values for x and y may physically be inacceptable when x and/or y are too short or too long from the chemical point of view.

The front term $(a_1\, b_2 - a_2\, b_1)$ in the determinant D of Eq. (A11) is explicitly

$$a_1\, b_2 - a_2\, b_1 = 2\,\frac{m_\mathrm{H}\, m'_\mathrm{H}}{M\, M'}\,(m_\mathrm{X}\, m'_\mathrm{Y} - m_\mathrm{Y}\, m'_\mathrm{X})\,. \tag{A12}$$

In the case of a terminal substitution $m_\mathrm{H} \to m'_\mathrm{H}$, when $m_\mathrm{X} = m'_\mathrm{X}$ and $m_\mathrm{Y} = m'_\mathrm{Y}$, the term $(a_1\, b_2 - a_2\, b_1)$ becomes zero, implying the solution for y^2 as

$$y_{1/2}^2 = \frac{B}{2A} = \frac{a_1\, d_2 - a_2\, d_1}{a_2\, c_1 - a_1\, c_2}\,. \tag{A13}$$

The corresponding solution for x^2 follows from Eq. (A5). Taking the positive square roots of x^2 and y^2, we obtain a unique solution of Eq. (A5) for the case of the terminal substitution $m_\mathrm{H} \to m'_\mathrm{H}$.